Pharmacological inhibition of STING reduces neuroinflammation-mediated damage post-traumatic brain injury

Amelia Fryer[1], Amar Abdullah[1], Frank Mobilio[1], Zachery Moore[1], Gang Zheng[2], Michael de Veer[2], Bruce Wong[1], Juliet Taylor[1], and Peter Crack[1]

[1]The University of Melbourne
[2]Monash University

August 4, 2023

Abstract

Background and Purpose: Traumatic brain injury (TBI) remains a major public health concern worldwide with unmet effective treatment. Stimulator of Interferon Genes (STING) protein and its downstream type-I Interferon (IFN) signaling are now appreciated to be involved in TBI pathogenesis. Compelling evidence have shown that STING and type-I IFNs are key in mediating detrimental neuroinflammatory response after TBI, exacerbating outcome. Therefore, pharmacological inhibition of STING presents a viable therapeutic opportunity in combating the detrimental neuroinflammatory response after TBI. Experimental Approach: This study investigated the neuroprotective effects of the small-molecule STING inhibitor C-176 in the controlled-cortical impact (CCI) mouse model of TBI in 10–12-week-old male mice. 30-minutes post-CCI surgery, a single 750nmol dose of C-176 or saline (vehicle) was administered intravenously. Analysis was conducted 2h- and 24h-post TBI. Key Results: Mice administered C-176 had significantly smaller cortical lesion area when compared to vehicle-treated mice 24h post-TBI. Quantitative temporal gait analysis conducted using DigiGait showed C-176 administration attenuated TBI-induced impairments in gait symmetry, stride frequency and forelimb stance width. C-176-treated mice displayed a significant reduction in striatal gene expression of pro-inflammatory cytokines TNF-α, IL-1β and CXCL10 compared to their vehicle-treated counterparts 2h post-TBI. Conclusion and Implications: This study demonstrates the neuroprotective activity of C-176 in ameliorating acute neuroinflammation and preventing white matter neurodegeneration post-TBI. This study highlights the therapeutic potential of small-molecule inhibitors targeting STING for the treatment of trauma induced inflammation and neuroprotective potential.

Title: Pharmacological inhibition of STING reduces neuroinflammation-mediated damage post-traumatic brain injury

Amelia L Fryer[1,+], Amar Abdullah,[1,2,+], Frank Mobilio[1], Zachery Moore[1,3], Gang Zheng[4], Michael de Veer[4], Bruce X Wong[1], Juliet M Taylor[1] and Peter J Crack[1]

[+]These authors contributed equally to this work.

Author affiliations:

[1] Neuropharmacology Laboratory, Department of Biochemistry and Pharmacology, University of Melbourne, Parkville, Melbourne 3010

[2] Department of Biological Sciences, School of Medical and Life Sciences, Sunway University, Selangor 47500, Malaysia

[3] Brain Cancer Laboratory, Personalised Oncology Division, The Walter and Eliza Hall Institute of Medical Research, Melbourne 3010, Australia

[4] Monash Biomedical Imaging, Monash University, Clayton 3168, Australia

Correspondence to: Professor Peter Crack

E-mail: pcrack@unimelb.edu.au

Running title : Blocking STING in neuroprotective post-TBI

Acknowledgements

We would like to thank Dr Andrew Jobling from the Department of Anatomy and Physiology at the University of Melbourne for the kind gift of the CX3Cr1 mice. The technical expertise in breeding and maintaining our mouse colonies by the School of Biomedical Sciences Bioresources facility at the University of Melbourne is gratefully acknowledged. The technical expertise and facilities of the National Imaging Facility (NIF) and Monash biomedical Imaging.

Competing interests

The authors report no competing interests.

Abstract

Background and Purpose:

Traumatic brain injury (TBI) remains a major public health concern worldwide with unmet effective treatment. Stimulator of Interferon Genes (STING) protein and its downstream type-I Interferon (IFN) signaling are now appreciated to be involved in TBI pathogenesis. Compelling evidence have shown that STING and type-I IFNs are key in mediating detrimental neuroinflammatory response after TBI, exacerbating outcome. Therefore, pharmacological inhibition of STING presents a viable therapeutic opportunity in combating the detrimental neuroinflammatory response after TBI.

Experimental Approach:

This study investigated the neuroprotective effects of the small-molecule STING inhibitor C-176 in the controlled-cortical impact (CCI) mouse model of TBI in 10–12-week-old male mice. 30-minutes post-CCI surgery, a single 750nmol dose of C-176 or saline (vehicle) was administered intravenously. Analysis was conducted 2h- and 24h-post TBI.

Key Results:

Mice administered C-176 had significantly smaller cortical lesion area when compared to vehicle-treated mice 24h post-TBI. Quantitative temporal gait analysis conducted using DigiGait showed C-176 administration attenuated TBI-induced impairments in gait symmetry, stride frequency and forelimb stance width. C-176-treated mice displayed a significant reduction in striatal gene expression of pro-inflammatory cytokines TNF-α, IL-1β and CXCL10 compared to their vehicle-treated counterparts 2h post-TBI.

Conclusion and Implications:

This study demonstrates the neuroprotective activity of C-176 in ameliorating acute neuroinflammation and preventing white matter neurodegeneration post-TBI. This study highlights the therapeutic potential of small-molecule inhibitors targeting STING for the treatment of trauma induced inflammation and neuroprotective potential.

Keywords: traumatic brain injury, STING, neuroinflammation, type-I interferon, neurodegeneration

Abbreviations:

AGS = Aicardi Goutières syndrome; ARRIVE= Animal Research: Reporting of*in vivo* Experiments; BBB = Blood brain barrier; CCI = Controlled cortical impact; c-di-GMP = Bis-(3'-5')-cyclic dimeric guanosine monophosphate; cGAMP = Cyclic adenosine monophosphate guanosine monophosphate; cGAS = Cyclic guanosine monophosphate AMP synthase; Ct = Cycle threshold; CX3CR1 = C-X3-C motif chemokine receptor 1; CXCL10 = C-X-C motif chemokine ligand 10; DAMP = Danger associated molecular pattern; DAPI = 4',6-diamino-2-phenylindole; ER = Endoplasmic reticulum; ERIS = Endoplasmic reticulum interferon stimulator; HRP = Horseradish peroxidase; IFNAR = Interferon alpha and beta receptor subunit; IKK = IκB kinase; IRF3 = Interferon regulatory factor 3; MITA = Mediator of IRF3 activation; OCT = optimal cutting temperature; PERK = Protein kinase R-like ER kinase; PFA = Paraformaldehyde; PVDF = Polyvinylidene fluoride; RARE = rapid acquisition, relaxation enhanced ; RIPA = Radioimmunoprecipitation; SAH = Subarachnoid haemorrhage; SDS = Sodium dodecyl sulphate; SLE = Systemic lupus erythematosus; STING = Stimulator of interferon genes; TBI = Traumatic brain injury; TBS = Tris-buffered saline; TBK1 = Tank binding kinase 1; TBST = Tris-buffered saline-tween; TMEM173 = Transmembrane protein 173

Bullet Point Summary

What is already known:

Aberrant neuroinflammation in a key-driver of secondary injury in TBI

Genetic deletion of stimulator of interferon genes (STING) is neuroprotective against TBI-induced inflammation in mice

What this study adds:

A novel use for small-molecule STING inhibitor C-176 in ameliorating TBI-induced neuroinflammation and neurodegeneration

Clinical significance:

Targeting the cGAS-STING pathway with small-molecule inhibitors minimises secondary injury post-TBI and displays neuroprotection.

Introduction

Traumatic brain injury (TBI) is a leading cause of death and disability in industrialised nations . TBI is a multifaceted pathology that varies in severity from a mild concussion to severe injury resulting in coma or death. Lasting neurobehavioral effects differ with severity of TBI and include attention deficits, poor cognition, development of anxiety or depression, antisocial behaviour, severe fatigue, and sleep disturbances . Current medical interventions for TBI primarily address the acute initial injury, resulting in a severe unmet need for new medical interventions targeting deleterious secondary injury cascades and conferring neuroprotection . Secondary injury in TBI is a complex array of interrelated molecular processes, such as excitotoxicity, necrosis and neuroinflammation, which all contribute to chronic neurodegeneration . This chronic neurodegeneration is implicated in the worsening of neurological function that is observed following TBI . Targeting secondary injury presents therapeutic potential to minimise progressive neuronal cell death and improve motor and cognitive outlook.

A key mediator implicated in the chronic neurodegeneration and worsened neurological function associated with secondary injury is neuroinflammation . The initial neuroinflammatory response following TBI is chiefly driven in response to the abundant cell death and BBB disruption that occurs as a result of the primary injury . Dysregulated neuroinflammation can prevail for weeks to years following TBI . This persistent neuroinflammation is strongly linked to the chronic neurodegeneration seen in TBI as well as a host of neurodegenerative conditions including stroke, Alzheimer's disease and Parkinson's disease . DAMPs released

by dying cells following TBI can result in the rapid release of pro-inflammatory molecules by microglia and astrocytes. These molecules include pro-inflammatory cytokines and chemokines such as type-I interferons (IFNs), tumour necrosis factor alpha (TNFα) and interleukin 1 beta (IL-1β) .

A critical pro-inflammatory mediator released by microglia and astrocytes to drive neuroinflammation are the type-I IFNs. Type-I IFNs are pleiotropic cytokines that have been implicated in the exacerbation of neuroinflammation following TBI and in the neurodegeneration observed in a host of other neurological disorders such as Aicardi-Goutiers syndrome (AGS), Alzheimer's disease and systemic lupus erythematosus (SLE) . Stimulator of interferon genes (STING), also known as transmembrane protein 173 (TMEM173), endoplasmic reticulum interferon stimulator (ERIS) and mediator of IRF3 activation (MITA), is an endoplasmic reticulum (ER) bound transmembrane adaptor protein . It plays a critical role in upregulating type-I IFN expression through the cGAS-STING pathway upon detection of cytosolic double-stranded DNA (dsDNA) .

dsDNA is recognised as a DAMP by the enzyme cyclic GMP-AMP synthase (cGAS) which initiates downstream signalling through STING, upregulating type-I IFN production . Once bound to dsDNA, cGAS facilitates the production of a cyclic dinucleotide, 2'5-cyclic adenosine monophosphate guanosine monophosphate (2'5'-cGAMP) from adenosine triphosphate (ATP) and guanosine triphosphate (GTP). 2'5'-cGAMP is the endogenous agonist of STING which induces STING oligomerisation . The activated STING oligomer translocates to the Golgi apparatus where it recruits and phosphorylates kinases tank binding kinase 1 (TBK1) and IκB kinase (IKK), forming multimeric dimers at the cytosolic domain of STING . Activated STING, TBK1 and IKK recruit and phosphorylate interferon regulatory factor 3 (IRF3) and nuclear factor kappa-light-chain-enhancer of activated B cells (NF-κB) at the C-terminal tail of STING . IRF3 and NF-κB are both promoters of type-I IFN transcription and once activated, they migrate to the nucleus, bind to IFN promoter regions, and potently upregulate type-I IFN production . Following activation, STING is rapidly degraded by lysosomes .

Aberrant STING activity is increasingly being appreciated to be damaging in contexts of acute and chronic sterile inflammation in neurodegenerative pathologies including stroke, Parkinson's disease, Huntington's disease, amyotrophic lateral sclerosis, ageing and TBI . Our group have previously established genetic deletion of STING signalling to be neuroprotective in the CCI mouse model of TBI with STING$^{-/-}$ mice displaying significantly smaller lesion size 24h post-TBI compared to wildtype mice . Work conducted by found that indirectly inhibiting STING signalling through the ER-stress sensor protein kinase R-like ER kinase (PERK) elicited similar neuroprotective outcomes in the CCI TBI mouse model. Furthermore, use of a STING agonist has been shown to exacerbate behavioural changes and pyroptosis in a rodent model of severe TBI , further suggesting that attenuating STING-mediated inflammation post-TBI is neuroprotective in mice.

As a targetable upstream modulator of type-I IFN signalling, the discovery of STING has generated new excitement in therapeutically harnessing inflammation . Unlike IFNAR1 and 2, STING is readily targetable using small-molecule agonists and antagonists, offering a new opportunity to therapeutically modulate type-I IFN production . Small-molecule nitrofuran derivative compounds have been found to inhibit STING activity by blocking activation-induced palmitoylation, which renders STING unable to form complexes in the Golgi apparatus in response to cyclic dinucleotide binding . Use of these small molecule inhibitors in mouse models of amyotrophic lateral sclerosis (ALS), subarachnoid haemorrhage SAH and severe TBI have observed neuroprotective effects, with mice displaying improvements in behaviour testing and a reduction in expression of proinflammatory cytokines and attenuated neuronal injury .

In this study, we employed the CCI model of mild TBI to evaluate the use of a small-molecule STING inhibitor (C-176) to confer neuroprotection post-mild TBI. Our group have previously confirmed that genetic deletion of STING in this mouse model was successful in reducing the lesion size. We hypothesise that small-molecule inhibition of STING will be protective against STING-mediated neuroinflammation. Here we report use of the C-176 post-CCI modelled TBI is neuroprotective by reducing white matter neurodegeneration around the lesion area and improving neurobehavioral outcomes.

Methods

Small-molecule STING inhibitor (C-176) preparation

Powdered n-(4-iodophenyl)-5-nitrofuran-2-carboxamide (C-176) (Enamine, Cat. No. EN300-6503757) was dissolved in dimethyl sulfoxide (DMSO) (Biochemical, Cat. No. BIOD0231) to achieve a final concentration of 10mM. Aliquots of stock solution were stored at -20°C until required.

Cell culture

BV2 cells were cultured in Dulbecco's modified eagle medium (DMEM) (Gibco, Cat. No. 11995-065) containing 5% foetal bovine serum (FBS) (Interpath, Cat. No. SFBSNZ5) and 1% penicillin-streptomycin (Life Technologies, Cat. No. 15070063) at 37 °C/5% CO2. Cells were plated in a 6-well plate at a density of 1 x 10^6 cells per well. Cells were pre-treated for 30 minutes in media containing 0.1-2μM C-176 or a DMSO vehicle. Following pre-treatment, c-di-GMP (Invivogen, Cat. No. tlrl-nacdg) was added to a final well concentration of 10-20μg/mL for 8 hours. Control wells were treated with an equivalent volume of endotoxin-free water. Following treatments, culture medium was removed, and wells were gently rinsed twice with ice cold phosphate-buffered saline (PBS) (Life Technologies, Cat. No. 18912014). Cells were scraped in PBS using a handheld cell scraper and placed in a cold Eppendorf tube. Samples were centrifuged at 3000g at 4°C for 10 minutes. Supernatants were removed and cell pellets stored at -80°C until required.

Animals

All animal experiments were carried out on adult male C57BL/6J mice or male and female CXCR1^{EGFP} mice aged 8-12 weeks old with an average body weight of 23 ± 3g. C57BL/6J Mice were sourced from the Animal Resources Centre (Western Australia) and CXCR1^{EGFP} were a gift from Dr Andrew Jobling (University of Melbourne) Mice were housed in groups of up to five per cage on a 12:12h light/dark cycle, with food and water provided *ad libitum* . All procedures, monitoring and reporting was performed in accordance with standard protocols approved by the University of Melbourne Animal Ethics Committee (Ethics ID # 1814589.4). All experimental work involving animals followed the ARRIVE guidelines for animal research .

Experimental groups

Mice were randomly assigned to receive either a sham or mild CCI surgery (TBI). 30 minutes following impact, a 200μL intravenous tail vein injection of 750nM C-176 (Enamine, Cat. No. EN300-6503757) diluted in phosphate-buffered saline (PBS) (Gibco, Cat. No. 18912-014) or a PBS vehicle was administered. Blinding of both the operator and data analysis was conducted by concealing the identity of the solution administered to mice post-TBI. Magnetic resonance imaging (MRI) and DigiGait analysis performed measuring lesion size and behavioural outcome respectively at 24h after TBI, with biochemical analysis performed at 2 and 24h after TBI. In this study the identity of each animal with respect to treatment was blinded to researchers who conducted the experiments and analysis.

Controlled cortical impact

The controlled cortical impact (CCI) procedure performed in this study was based on standard protocols as previously described and reported by our group . This model of TBI was selected as it is well documented to model secondary-injury inflammatory processes in addition to its high degree of reproducibility (Osier & Dixon 2016). Mice were anesthetised with ketamine (100mg/kg, Parnell)/xylazine (10mg/kg, Sigma, Cat. No. X-1251) via intra-peritoneal injection. A sagittal incision was made to expose the skull before a 2mm diameter craniotomy was performed using a handheld electrical drill (Dremel, 10.8V) at 2.5mm lateral the midline and 1.5mm posterior to the bregma to expose the right parietal cortex. The mice were restrained

in a stereotaxic frame device for the injury to be delivered using a 2mm flat computer-controlled impactor (LinMot-Talk 1100). An impact 1.5mm deep was applied to the exposed cortex at a velocity of 1m/s and a dwell time of 100ms. The skull flap previously removed during the craniometry was replaced over the exposed cortex and the sagittal incision was sutured by hand using wax coated braided silk (Covidien, Cat. No. GS-832). 30 mins following successful CCI, mice were administered either C-176 or PBS intravenously. Post-surgery, all mice were administered buprenorphine (0.6mg/kg, Lyppard Australia Pty Ltd) intraperitonially and placed on a heat mat to recover from anaesthesia and their condition was monitored hourly over 6 hours and the subsequent morning. Sham mice underwent identical anaesthesia, sagittal incision and craniometry as TBI mice, omitting the impact by the computer-controlled impactor. The mice were housed for 2- or 24-hours following surgery and euthanised via cervical dislocation before subsequent analysis.

MRI acquisition

MRI scans were performed for this study using a hybrid Agilent 9.4 Tesla small animal MRI scanner using Bruker imaging hardware and software (Monash Biomedical Imaging) to quantify the progression of tissue damage. Mice were anesthetized with 3% isoflurane in medical-grade oxygen. Anesthesia was maintained throughout scanning with 0.25 to 1.5% isoflurane through a nosecone placed over the animal's snout and anesthetized animals were laid supine on a purpose-built small-animal holder and their heads fixed into position with ear and bite bars and respiration rate was continuously monitored. A Bruker mouse heart surface receiver coil was placed under the animals' head and the cradle was inserted into a Bruker 86mm transmitter coil fixed inside an Agilent SGRAD 120/HD/S gradient set for imaging. The MRI protocol consisted of a three-plane localizer sequence followed by multiecho T2 and diffusion-weighted sequences. The total scanning time was kept to <1 h per animal. Multiecho T2 -weighted images were acquired using a rapid acquisition, relaxation enhanced (RARE) sequence with RARE factor = 2; repetition time = 2500 ms; effective echo time (TEeff) = 10, 30, 50, 70, 90, and 110 ms; field-of-view = 1.6 Å 1.6 cm^2; matrix = 192 A 192; and 24 slices with thickness = 0.5 mm. Volumetric analysis was carried out on T2-weighted images using MRIcroGL software, available from www.nitrc.org/projects/mricrogl .

Gait analysis

The gait dynamics of the mice pre-and post-surgery were recorded non-invasively using a DigiGait^{TM} apparatus (v11.5, Mouse Specifics^{TM}). The apparatus consists of a transparent conveyor belt over a recording device to capture the gait dynamics of the mice from underneath the belt. The belt was set to operate at a fixed speed of 15cm/s at an incline of 0 degrees. Light fur and tails were coloured with black ink to reduce noise in recording. Mice were given one 'test run' prior to recording. The gait dynamics of the mice were recorded in triplicate over a running period of 4 seconds for each recording. Gait indices were quantified using the DigiGait^{TM} Imaging System. The duration of each gait interval, which includes the duration of the stride, stance, swing, braking and propulsion phase (seconds) was used for gait analysis (Table 1).

Western blot analysis

Protein isolation

Protein extraction from cells was conducted using radioimmunoprecipitation assay (RIPA) lysis buffer comprising of 50mM tris-HCL, 150 mM NaCl, 1% Triton X-100, 0.1% sodium dodecyl sulphate (SDS), 0.5% sodium deoxycholate, 2mM ethylenediaminetetraacetic acid (EDTA), half of a cOmplete protease inhibitor cocktail tablet (Sigma-Aldrich, Cat. No. 11697498001) and one PhosSTOP phosphatase inhibitor cocktail tablet (Roche, Cat. No. 04906837001). 50µL of buffer was added to each cell pellet, samples were sonicated for 10 pulses at 10% followed by incubation on ice for 30 minutes before storage at -80°C.

Mouse brains were dissected into ipsilateral and contralateral hemispheres and the cortex and striatal regions were isolated from each hemisphere. Samples were snap-frozen in liquid nitrogen and finely ground using a mortar and pestle. The ground sample was then further mechanically homogenised using a silicon microtube

pestle at a tissue weight to homogenisation buffer ratio of 1:4. The homogenisation buffer comprised of 10% tris buffer (50mM tris hydrochloride (Chem-supply, Cat. No. BIOTB0103) and 150mM sodium chloride (Chem-supply, Cat. No. SA046)), 1% triton x-100 (Sigma-Aldrich, Cat. No. T8787), one cOmplete protease inhibitor cocktail tablet (Sigma-Aldrich, Cat. No. 11697498001) and half of a PhosSTOP phosphatase inhibitor cocktail tablet (Roche, Cat. No. 04906837001). The homogenised samples were placed on a microtube roller for two hours at 4degC before centrifugation at 2000g for 10 minutes Supernatants were placed in fresh tubes and stored at -80degC for protein analysis.

Western blot

Protein concentration was determined by Bradford assay. Isolated proteins were incubated with 2X Novex tris-glycine SDS sample buffer (Thermo, Cat. No. LC2676) containing 5% 2-mercaptoethanol (Sigma-Aldrich, Cat. No. M3148) for 5 minutes at 90degC. 20-40µg of protein was resolved on 10% acrylamide SDS-0 (PAGE) gels. Gels were transferred to polyvinylidene fluoride (PVDF) membranes (Bio-Rad, Cat. No. 1704272) using a Trans-Blot® SD semi-dry transfer cell (Bio-Rad). Membranes were then blocked in 5% w/v skim milk in tris-buffered saline (TBS) with 0.05% Tween-20 (Sigma, Cat. No. P1379) (TBS-T) for one hour, followed by an overnight incubation at 4°C with primary antibody (Supplementary Table 1) diluted in 5% w/v skim milk. The membranes were washed three times for 10 minutes each with TBS-T and incubated with horseradish peroxidase (HRP) conjugated secondary antibody (Supplementary Table 2) in 5% w/v skim milk for one hour at room temperature. Membranes were washed again with TBS-T and signals detected using an Amersham ECL prime western blotting detection kit (GE Healthcare, Cat. No. GEHERPN2232) and imaged using a ChemiDoc imaging XRS+ system (Bio-Rad). Band intensity was measured using Image Lab software (Bio-Rad, Version 6.0.1) and normalised to the β-actin loading control. Values are presented as band intensity relative to β-actin.

Quantitative real-time PCR

RNA isolation

Brains were dissected into ipsilateral and contralateral hemispheres and cortex and striatal regions isolated from each hemisphere 24h after TBI and sham surgery. The samples were snap frozen in liquid nitrogen and mechanically ground. Samples were mechanically homogenised in 1mL TRIzol using a 21" gauge needle. One-part degassed chloroform was added to 5 parts sample in TRIzol solution and samples were spun at 12,000g for 15 minutes. The aqueous layer was removed and transferred to filter columns from an Illustra RNAspin mini isolation kit (GE Healthcare, Cat. No. 25050071). Further purification and DNase treatment of the RNA was conducted as per kit instructions. RNA was eluted in 50µL RNase-free H_2O, and the eluate reapplied to the spin column again and re-spun. Concentration and purity (260/280nm and 260/230nm) of RNA was measured using a NanoDrop 1000 spectrophotometer.

QPCR

cDNA was diluted 1:10 with RNase-free water. The TaqMan or SYBR Green detection system was used with commercially available probes (Supplementary Table 3 for TaqMan and Supplementary Table 4 for SYBR Green). QPCR analysis was conducted using a QuantStudio 6 real-time PCR system (Invitrogen). Results were analysed using QuantStudio software (Life Technologies, Version 1.1). Cycle threshold (Ct) values were normalised to the housekeeping gene Glyceraldehyde-3-phosphate dehydrogenase (GAPDH). Relative gene expression was calculated using the comparative C_T method .

Immunohistochemistry

Mice were anesthetised via intraperitoneal administration of ketamine/xylazine (100mg/kg (Parnell)/xylazine (10mg/kg, Sigma Cat. No. #X-1251) and cardiac perfused with ice cold PBS followed by ice cold 4% paraformaldehyde (PFA) (Scharlau, Cat. No. PA00950500). Isolated brains were post-fixed in 5mL of 4% PFA overnight at 4°C, then placed 30% sucrose solution (Chem-supply, Cat. No. SA030) for 48 hours. The brains were then embedded in optimal cutting temperature media (OCT) (Sakura, Cat. No.

4583) and coronally sectioned at a thickness of 30µm. Sections were washed three times with PBS on a rocker at 20RPM for 5 minutes each followed by 2-hour incubation in blocking buffer containing 10% goat serum (Sigma-Aldrich, Cat. No. G9023) and 1% Tween-20 (Sigma-Aldrich, Cat. No. P1379). Following blocking, sections were rinsed in PBS followed by overnight incubation with primary antibody (Supplementary Table 5) on a rocker at 20RPM at 4°C. Sections were then rinsed with PBS and incubated at room temperature for one hour with secondary antibodies (Supplementary Table 6). Sections were again rinsed three times with PBS followed by one rinse with milliQ H_20 before being mounted onto Superfrost plus slides (Thermo Scientific, Cat. No. SF41296SP) with Vectashield HardSet antifade mounting medium with DAPI (Abacus ALS, Cat. No. H-1500). Slides were imaged using a Zeiss Observer Z1 widefield microscope and Zen 2.6 (Zeiss, blue edition) software.

Microglial morphological analysis

The quantification of microglial morphology performed in this study was based on a protocol previously described and reported by our group . 30µm sagittal brain sections were collected and imaged using Zeiss Observer Z1 widefield microscope with 10X magnification. 3-5 images were taken at the perilesional cortex and at the corresponding location on the contralateral cortex. Images underwent maximum intensity projections before analysis. Images were analysed using a proprietary spanning tree path finding based algorithm with a minimum of 50 microglia per image analysed . Trace images were then analysed on Matlab v2013b using built-in functions. To ensure that only cells with visible major branches were included in the analysis, cells overlapped with each other or had contact with the image border were excluded from analysis.

Data and Statistical Analysis

The data and statistical analysis comply with the recommendations on experimental design and analysis in pharmacology . All statistical analysis was conducted using GraphPad Prism version 8.4.2 for Windows. Data is presented as mean ± standard error of the mean (SEM). Sample size was determined by power analysis. A variance was set at 15% to determine a 25% significant difference will require a group of 8 or more animals for behavioral and infarct size analysis. For comparisons between two treatment groups, a two-tailed student t-test was used. For comparisons between three or more treatment groups, a one-way ANOVA with a Tukey's post-hoc multiple comparisons test was used. p-values less than 0.05 were deemed statistically significant.

Results

C-176 attenuates STING activation in BV2 cells

To assess the efficacy of C-176 in inhibiting STING activation, we pre-treated BV2 microglia-like cells with 0.1-2µM of C-176 followed by an 8-hour incubation with 10-20µg of STING agonist cyclic-di-GMP (Fig 1). Inhibition of c-di-GMP induced STING and TBK1 phosphorylation was observed following incubation with 0.1, 1 and 2µM C-176, with complete inhibition of STING and TBK1 phosphorylation at a concentration of 2µM of C-176 (Fig 1).

C-176 administration post-TBI reduces cortical lesion size

The effect of C-176 on trauma-induced neuroinflammation was assessed*in vivo* using the CCI model of mild TBI. MRI imaging was conducted to evaluate cortical damage 24h post-TBI in mice intravenously injected 30 minutes post-TBI with a single 750nmol dose of C-176 (C-176) or a saline-vehicle control (Vehicle). Quantification of the lesion area revealed that mice treated with C-176 had significantly reduced area of damage in the cortex 24h post-TBI compared to vehicle-treated TBI mice (Fig 2).

Treatment with 750nmol C-176 post-injury rescues gait disturbances in mice 24h-post TBI

This study conducted a quantitative temporal gait analysis using to gauge alterations in neurobehavioral activity following TBI in mice. Changes in gait parameters were measured using DigiGait (parameter definitions provided in Table 1). C-176 administration attenuated TBI-induced impairments in stride frequency (Fig 3E and Fig 4E) and forelimb stance width (Fig 3D), in addition to restoring time spent in forelimb and hindlimb stance phase and stride phase to values similar to sham and statistically longer than vehicle-treated TBI mice (Fig 3B-C and Fig 4B-C).

Furthermore, the vehicle treated TBI mice treated displayed an elevated gait symmetry ratio compared to sham (Fig 3F). A gait symmetry value of 1 indicates co-ordinated movement in both the left and right side of the body. The gait symmetry measured in mice treated with C-176 after TBI was closer to 1 compared to vehicle-treated mice and was not statistically different to sham mice (Fig 3F). The sham and vehicle treated TBI mice had similar hindlimb stance width and mice treated with C-176 after TBI exhibited a narrower hindlimb stance width (Fig 4E).

C-176 on STING expression after TBI

To evaluate the effect of single-dose C-176 administration on STING-mediated neuroinflammation, 2h and 24h post-TBI, protein and mRNA expression of STING (TMEM173) and downstream mediators TBK1 and IRF3 was measured using western blot and qPCR. Mice treated with C-176 did not display significant alterations to the expression of STING mRNA expression in the cortex and striatum when compared to vehicle-treated mice at both 2h and 24h post-TBI (Sup Fig 2F, Sup Fig 3F). IRF3 mRNA expression in the striatum of C-176 treated mice significantly increased 2h-post TBI when compared to vehicle-treated mice (Sup fig. 2G) and remained relatively unchanged 24h post-TBI (Sup Fig 3G). Western blot analysis revealed that there were no significant changes in cortical STING protein expression observed 2h-post TBI in C-176-treated mice compared to sham or vehicle-treated mice (Sup fig 2C). Interestingly, C-176 treated mice displayed significantly attenuated total TBK1 expression in the striatum 2h-post-TBI compared to sham (Sup Fig 2C). Both C-176 and vehicle treated mice had a reduction in the protein expression of STING and total and phosphorylated TBK1 in the cortex and striatum compared to sham 24h post-TBI (Sup Fig 3C-E).

C-176 does not alter microglial phenotype

Since we identified an alteration to STING mRNA expression and TBK1 and p-TBK1 expression in vehicle treated mice 24h post-TBI, we wanted to elucidate if these changes also resulted in altered microglial activity. Immunohistochemical analysis was conducted on CX3CR1^{eGFP} mice which have fluorescently tagged microglia. Morphological analysis was conducted on CX3CR1^{eGFP} mice 24h-post TBI to quantify any phenotypical changes to the microglia that could indicate alterations to the inflammatory environment in the CNS. STING was found to strongly colocalise with CX3CR1-tagged microglia 2h-post TBI (Fig 5). There was a small increase in soma size detected post-TBI compared to the microglia contralateral to the TBI-lesion, however, no differences in total branch length, cell area or soma area were observed between vehicle-treated and C-176 treated mice post-TBI (Fig 6).

C-176 reduces TBI-induced proinflammatory cytokine response 2h-post injury

To elucidate the effect of C-176 on the neuroinflammatory milieu post-TBI, gene expression of pro-inflammatory markers intimately related to the type-I IFN response was measured in the ipsilateral cortex and striatum region of the brain at 2h and 24h-post TBI (Fig 7). Administration of C-176 significantly attenuated cortical expression of*CXCL10* 2h-post TBI (Fig 7Av) compared to vehicle-treated mice and did not have a marked effect on cortical expression of the other pro-inflammatory markers measured (Figure 7Ai-iv,vi). C-176-treated mice displayed a significant reduction in striatal gene expression of pro-inflammatory cytokines *TNΦ-α, IΛ-1β* and *CXCL10*compared to their vehicle-treated counterparts at 2h post-TBI (Fig 7Ai,iii-,v).Vehicle-treated mice 24h post-TBI displayed significantly elevated expression of *IL-1* β, *TNΦ-α* and *CXCL10* in both the cortex and the striatum compared to sham (Fig 7i, iii, v).*IL-6* and *iNOS* expression increased in the vehicle-treated TBI mice in the cortex (Fig 7B ii, iv). C-176 treated mice displayed

significantly increased expression of *TNΦ-α* in both the cortex and the striatum (Fig 7Biii) and *CXCL10* in the cortex compared to sham (Fig 7Bv). No significant difference in the expression of the pro-inflammatory markers measured was detected between the vehicle-treated mice and C-176 treated mice 24h-post TBI (Fig 7B).

Discussion and Conclusions

Traumatic brain injury is often referred to as a 'silent epidemic', causing debilitating neurological deficits to millions of people globally each year (James et al., 2019). Treatments limiting the damage caused by secondary injury processes following TBI is an area of severe unmet medical need . Medical intervention is limited to stabilization of the patient via barbiturate coma and decompressive surgical intervention. The patient has little scope to improve neurological function and an extremely decreased quality of life . After injury the neural cells die from physical damage, eliciting a sequence of events that creates a neuroinflammatory microenvironment which prevents recovery. Neurodegeneration driven by complex, chronic and dysregulated neuroinflammation is particularly detrimental to the neurological recovery after TBI . cGAS-STING-IFN signalling is increasingly being appreciated as a driver of this neuroinflammation in rodent models of TBI . Here we examine if pharmacological inhibition of STING can attenuate neuroinflammation and neurodegeneration post-TBI and lead to neuroprotection and improved behavioural outcome.

We firstly identified that C-176 can successfully inhibit STING activation in glial cells with the use BV2 microglia-like cells (Fig 1). Importantly, this identified that C-176 was targeting STING activation. We then employed a single-dose administration of this STING inhibitor in our mouse model of mild-TBI. It was evident that single-dose administration of C-176 post-TBI in our mouse model was able to confer neuroprotection. The timepoint of 30 minutes was chosen in this study to represent the 'golden hour' in which intervention for TBI may have the most beneficial effects. It is important to note that in developed countries such as the England and Wales, the median time to intervention for patients post-severe and moderate TBI is 0.5-0.9 hours Mice treated with C-176 displayed significantly smaller lesion areas 24h-post TBI (Fig 2). These results are comparable with previous findings by our group using STING$^{-/-}$ mice, which highlighted that deletion of STING resulted in neuroprotection after TBI . These results are also consistent with the work conducted by Zhang et al (2022), where administration of C-176 in a rat model of severe TBI showed attenuated neuronal loss around the lesion site 24h-post TBI. Additionally, use of C-176 in a mouse model of stroke was also found to significantly reduce infarct size 24h after stroke modelling . Our neurobehavioral findings further confirm the neuroprotective capability of C-176 post-TBI. We found that TBI-induced gait deficits were reversed following C-176 administration (Fig 3 and 4). Studies using C-176 in rodent models of severe TBI and ischemic stroke have all found similar improvements in neurological and cognitive function suggesting that this compound could be beneficial in alleviating acute neurological symptoms .

Previous studies have identified microglia to key a key source of STING activity in the CNS . We were able to confirm that STING expression was predominately located in microglial cells post-TBI (Fig 5). We are the first to assess microglial morphology following administration of C-176 and found that administration of C-176 did not elicit any morphological changes in the perilesional microglia between C-176-treated mice and their vehicle counterparts (Fig 6.). Work conducted by Zhang et al (2022) found that administration of C-176 reduced the colocalization of STING in microglia and astrocytes 32 days post-severe TBI. This suggests that there may be more significant morphological and biochemical changes may be occurring in microglia at a timepoint later than the one used in the present study (24h-post TBI). This result also highlights that early administration of a STING inhibitor may be important in limiting the morphological and biochemical changes that occur in microglia after TBI.

Mild TBI and single-dose administration of C-176 were found to alter the neuroinflammatory profile in the cortex and striatum 2 and 24h-post TBI. The anti-inflammatory effects of the C-176 post-TBI were observed acutely post-injury and had most observable attenuation of expression of pro-inflammatory genes *CXCL10* and *TNΦ-α* in the striatum 2h-post injury (Fig 7Aiii,v). Previous work by our group have demonstrated that

hematopoietic cells play a key role in the neuroinflammatory response in this model. Neuroinflammation is a hallmark of various neurological disorders, including TBI . Activation of the STING pathway in microglia and astrocytes contributes significantly to the production of pro-inflammatory mediators, such as TNF-α, IL-1β, and IL-6, which exacerbate neuroinflammation . The STING pathway has been shown to amplify the inflammatory response by inducing the nuclear factor-kappa B (NF-κB) pathway, a master regulator of inflammation, and inflammasome activation . Future work would investigate if C-176 is acting through these peripheral cells to elicit the neuroprotective anti-inflammatory effect we have observed.

We did not observe changes to the total protein expression of STING 2h-following TBI or C-176 administration (Sup Fig 2). Interestingly we found significantly attenuated STING, TBK1 and p-TBK1 24h-post TBI. We did not however find any significant changes between the vehicle-treated TBI mice and the C-176 treated mice. Work conducted by Zhao et al (2022) using C-176 in a rat model of severe TBI found increased p-TBK1 and TBK1 expression in isolated hippocampus 24h-post TBI and C-176 was found to significantly decrease this p-TBK1 expression. We did observe an increase in the mRNA expression of STING (TMEM173) in the cortex and striatum of the vehicle-treated TBI mice 24h-post TBI and not at 2h-post TBI. Together this highlights the temporal sensitivity of STING activation in the CNS. Future studies should evaluate STING activation at later timepoints in addition to evaluating the expression in isolated hippocampus to further understand the effect of C-176 on STING activation in the CNS post-TBI.

Future studies will explore the pharmacokinetics of C-176 to address if its neuroprotective anti-inflammatory is occurring solely in the CNS or if it is acting on STING in peripheral immune cells. Furthermore, C-176 has been recorded to possess a short half-life when used in mice, thereby reinforcing the need to explore dosage frequency, concentration and timing to achieve optimal therapeutic effect (Haag et al., 2018). Future studies can provide more insight into the therapeutic window of using STING inhibitors by broadening the dosage concentration, frequency, timing, and route of administration tested in this mouse model.

This study has demonstrated a neuroprotective role of small-molecule inhibition of STING following mild TBI in mice, supporting additional studies investigating the therapeutic intervention of this pathway to address the severe unmet medical need of limiting the cell damage and functional deficits in TBI patients. The social and economic burden of brain injury is considerable to the community. New pharmacological tools are urgently needed to help delineate the neuroinflammatory pathways post TBI and determine the most advantageous therapeutic window for the acute treatment of TBI.

Data Availability

The data that support the findings of this study are available from the corresponding author upon request.

Funding

Funding support for this work was provided by the National Health and Medical Research Council (NHMRC) and The Brain Foundation.

Declaration of Transparency and Scientific Rigor

This Declaration acknowledges that this paper adheres to the principles for transparent reporting and scientific rigor of preclinical research as stated in the *BJP* guidelines for Design and Analysis, Immunoblotting and Immunohistochemistry and Animal Experimentation and as recommended by funding agencies, publishers and other organisations engaged with supporting research.

Supplementary material

The supplementary material for this article can be found online.

References

Figure Legends

Figure 1. C-176 inhibits cyclic di-nucleotide (CDN) mediated STING activation.

Inhibition of STING and TBK1 phosphorylation occurs in BV2 microglia-like cells pre-treated for 30 minutes with STING inhibitor C-176 and treated for 8 hours with 10-20μg of c-di-GMP. **(A)**Protein expression analysed by western blot. Densitometric analysis**(B-C)** was performed to quantitate expression of p-STING relative to STING and p-TBK1 relative to TBK1. Protein expression was measured as ratio of band intensity and β-actin loading control. The expression of p-STING **(B)** and p-TBK1 **(C)** was made relative to total protein expression of STING and TBK1 respectively. All data is expressed as mean ± SEM. STING phosphorylation was significantly increased following treatment with 10μg/mL (p=0010) and 20μg/mL (p<0.0001) of c-di-GMP compared to untreated vehicle. Treatment with 2μM C-176 completely ablated c-di-GMP induced phosphorylation of STING. n = 5. Significance determined by two-way ANOVA followed by a Bonferroni's multiple comparison test within each dose of C-176. *p<0.05, **p<0.01, ***p<0.001, ****p<0.0001

Figure 2. Administration of C-176 reduces TBI-induced brain lesion

MRI T2 images from C57BL/6 mice showing TBI lesion 24h-post injury**(A)** . Mild TBI was modelled using a controlled cortical impactor. 30-minutes post-TBI, mice were intravenously administered a vehicle or C-176. Sham mice underwent identical surgery omitting the TBI. Mice administered C-176 post-TBI had significantly reduced lesion volumes 24h after injury (*p=0.01) **(B)** . Data represents mean ± SEM, n=8-9 animals per group.

Figure 3. C-176 significantly improves left forelimb gait deficits 24h post-TBI.

Quantitative temporal gait parameters of mice were measured using DigiGait imaging and analysis software 24h after 1.5mm impact CCI surgery (TBI) and no impact (sham). No change in **(A)** swing duration was observed. Significant improvements found in **(B)**stance (p<0.0001) and **(C)** stride duration (p=0.0032),**(D)** stride frequency (p=0.0011), **(E)** forelimb stance width (p=0.0254) and **(F)** gait symmetry (p=0.0237) in TBI mice treated with STING inhibitor (C-176) compared to TBI mice treated with a vehicle. Sham n = 8, TBI-vehicle n = 10, TBI-C-176 n = 13. Data is presented as mean +- SEM. Significance determined by one-way ANOVA with Tukey's multiple comparison test. *P< 0.05, **P<0.01, ***P<0.001, ****P<0.0001.

Figure 4. C-176 significantly improves left hindlimb gait deficits 24h post-TBI.

Quantitative temporal gait parameters of mice were measured using DigiGait imaging and analysis software 24h after 1.5mm impact CCI surgery (TBI) and no impact (sham). No change in swing duration between treatment groups was observed **(A)** . Significant improvements found in **(B)** stance (p=0.0005) and **(C)** stride duration (p=0.0037), and **(E)** stride frequency (p=0.0041) in TBI mice treated with STING inhibitor (C-176) compared to TBI mice treated a vehicle. **(D)** Hindlimb stance width in C-176 treated mice significantly lower than sham (p=0.0052) and vehicle treated TBI mice (p<0.0001). Sham n = 8, TBI-vehicle n = 10, TBI-C-176 n = 13. Data is presented as mean +- SEM. Significance determined by one-way ANOVA with Tukey's multiple comparison test. *P< 0.05, **P<0.01, ***P<0.001, ****P<0.0001

Figure 5. STING expression colocalises with microglia 2h-post TBI.

Representative immunofluorescence images of STING (red) and GFP-tagged CX3CR1 microglia (green) taken around lesion area 2h-post TBI. 30 minutes following TBI, mice were administered a saline vehicle**(A)**

or a single dose of C-176 **(B).** Images taken on Zeiss Axio Observer 7.1 widefield microscope at 20X objective. Scale bar: 25μm

Figure 6. Administration of C-176 does not alter microglial morphology 24h-post TBI.

30μm thick brain sections of CX3CR1^{eGFP} mice subjected to CCI TBI. Representative images are shown for the ipsilateral and contralateral cortex of vehicle-treated **(A)** and C-176-treated**(B)** mice with an overview of the skeletonising process employed using a minimum spanning tree algorithm to measure morphological characteristics. Administration of C-176 did not significantly alter**(C)** total branch length **(D),** cell area or **(E)**soma area of perilesional microglia compared to vehicle treated mice 24h-post TBI. Each data point is an average of 200-500 cells. Scale bar = 50μm. n=5 for each group.

Figure 7. Gene expression of pro-inflammatory markers 2h and 24h following TBI and C-176 administration in mice.

Gene expression of pro-inflammatory markers *IΛ-1β* **(A)** ,*TNF-[?]* **(B),** *CXCL10* **(C),** *IL-6***(D),** *iNOS* **(E)** and *TΓΦ-β* **(F)**measured by qPCR in the ipsilateral cortex or striatal region of the brain 2h and 24h post controlled-cortical impact modelled TBI. All data is presented as mean ± SEM. 2h-TBI n = 6, 24h-TBI n = 9. Significance was determined for the cortex and striatum separately using a one-way ANOVA and Tukey's multiple comparison test. *p [?] 0.05, **p [?] 0.01, ***p [?] 0.001, ****p < 0.0001.

Supplementary figure 1. Validation of STING antibody

Brain lysate extracted from isolated cortex or striatum of wildtype (WT) or STING$^{-/-}$ C57Bl/6 mice. Total STING expression was detected using western blot. A single band was observed at approximately 37kDa in the WT lanes and was absent in STING$^{-/-}$

Supplementary Figure 2. STING, TBK1 and IRF3 expression 2h post-TBI and C-176 administration.

Representative images of STING, p-TBK1 and TBK1 protein expression the ipsilateral cortex and striatum of mouse brains 2h after controlled-cortical impact modelling of TBI or sham surgery as detected by western blot **(A-B)** . Quantification of total STING**(C),** phospho-TBK1 **(D)** and total TBK1 **(E)**protein expression relative to β-actin loading control. No significant changes in the expression of **(C)** STING and **(D)** p-TBK1 were observed following TBI and C-176 administration compared to sham mice. TBI-mice treated with C-176 had a significantly lower expression of **(E)** total TBK1 compared to sham mice (p=0.026). Gene expression analysis by qPCR revealed no significant changes in the expression of TMEM173 **(F)** in the ipsilateral cortex and striatum and IRF3 **(G)** in the ipsilateral striatum 2h-post TBI. TBI-mice treated with C-176 had significantly elevated IRF3 expression compared to sham (p<00001) and vehicle-treated TBI-mice (p<0.00001). All data is expressed as mean ± SEM. Significance determined using a one-way ANOVA with Tukey's multiple comparison test. **p [?] 0.01, *** p [?] 0.001. n = 7 for each treatment group.

Supplementary Figure 3. STING, TBK1 and IRF3 expression 24h post-TBI and C-176 administration.

Representative images of STING, p-TBK1 and TBK1 protein expression the ipsilateral cortex and striatum of mouse brains 24h after controlled-cortical impact modelling of TBI or sham surgery as detected by western blot **(A-B)** . Quantification of total STING**(C),** phospho-TBK1 **(D**), and total TBK1 **(E)**protein expression relative to β-actin loading control. Protein expression of STING **(C)** was significantly decreased in the cortex and striatum of TBI mice treated with vehicle (cortex p=0.0050, striatum p=0.0335 and C-176-treated mice (cortex p=0.0062, striatum p=0.0064) when compared to sham mice 24h-post TBI. No significant difference was observed in the expression of STING between the vehicle-treated and the C-176 treated TBI mice. P-TBK1 expression was significantly decreased in the cortex and striatum of both the vehicle-treated (cortex p=0.0054, striatum p=0.0202) and the C-176 treated mice (cortex p=0.0350, striatum p=0.0480) compared to sham mice. Gene expression analysis by qPCR revealed an increased expression of TMEM173 **(F)** 24h-post TBI in the cortex of both the vehicle treated mice (p=0.0002) and the C-176 treated mice (p=0.0057)

compared to sham. Vehicle treated mice also displayed an increased expression of TMEM173 (p=0.0005). No significant change in the expression of IRF3**(G)** was detected between all treatment groups. All data is expressed as mean ± SEM. Significance determined using a one-way ANOVA with Tukey's multiple comparison test. **p [?] 0.01, *** p [?] 0.001. n = 9 for each treatment group.

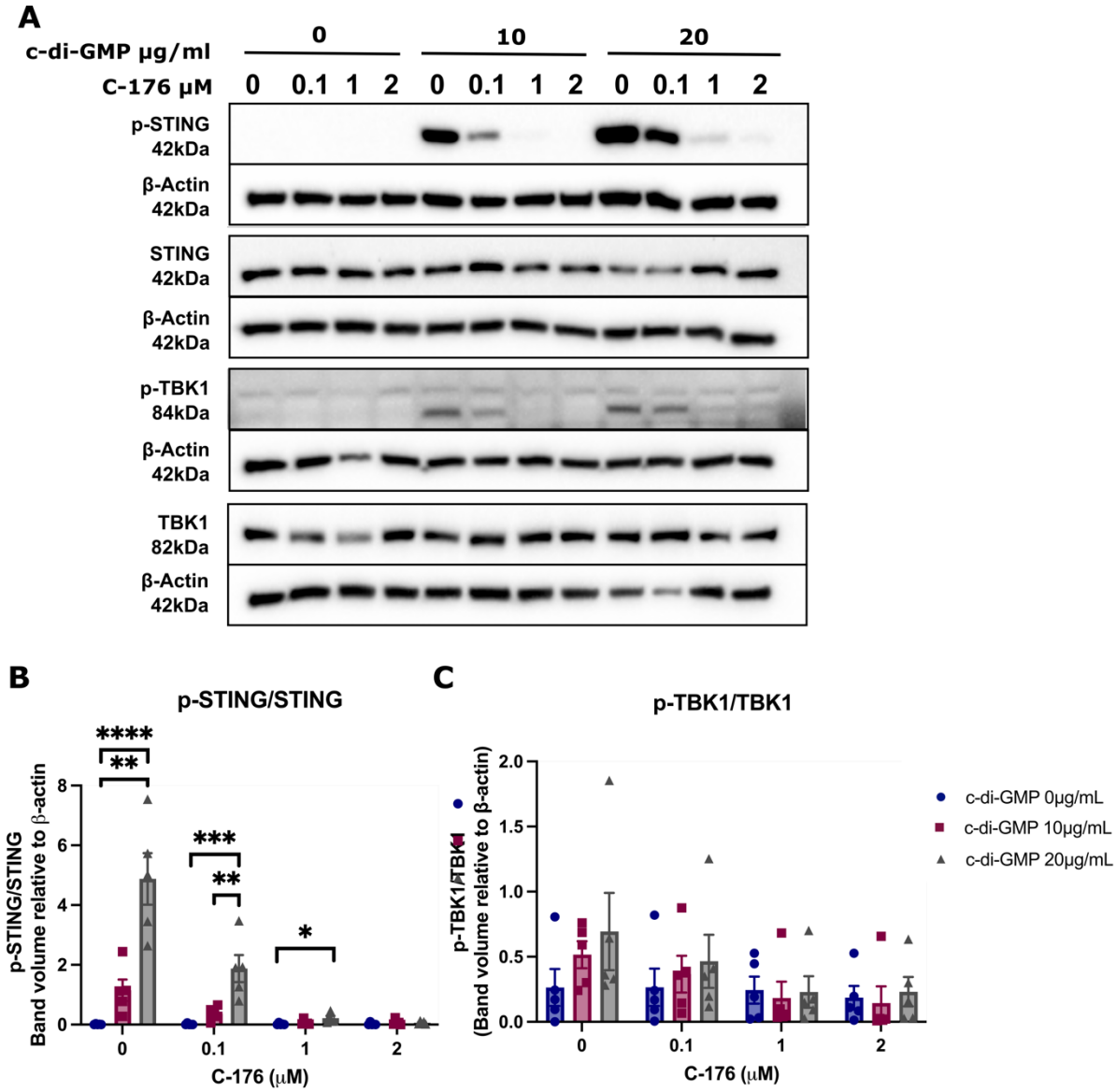

Figure 1. C-176 inhibits cyclic di-nucleotide (CDN) mediated STING activation.

Inhibition of STING and TBK1 phosphorylation occurs in BV2 microglia-like cells pre-treated for 30 minutes with STING inhibitor C-176 and treated for 8 hours with 10-20µg of c-di-GMP. (A) Protein expression analysed by western blot. Densitometric analysis (B-C) was performed to quantitate expression of p-STING relative to STING and p-TBK1 relative to TBK1. Protein expression was measured as ratio of band intensity and β-actin loading control. The expression of p-STING (B) and p-TBK1 (C) was made relative to total protein expression of STING and TBK1 respectively. All data is expressed as mean ± SEM. STING phosphorylation was significantly increased following treatment with 10µg/mL ($p=0010$) and 20µg/mL ($p<0.0001$) of c-di-GMP compared to untreated vehicle. Treatment with 2µM C-176 completely ablated c-di-GMP induced phosphorylation of STING. n = 5. Significance determined by two-way ANOVA followed by a Bonferroni's multiple comparison test within each dose of C-176. *$p<0.05$, **$p<0.01$, ***$p<0.001$, ****$p<0.0001$

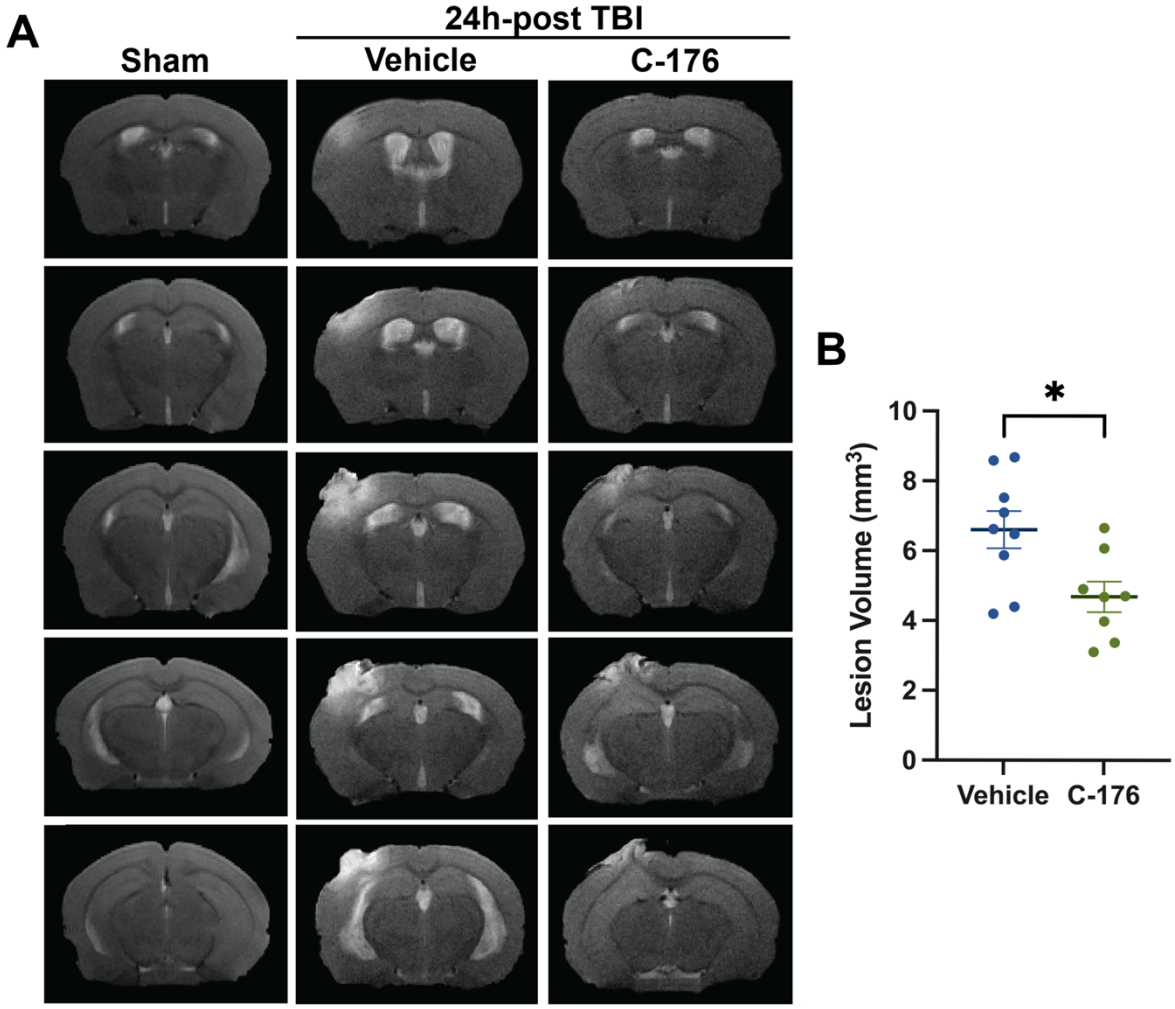

Figure 2. Administration of C-176 reduces TBI-induced brain lesion

MRI T2 images from C57BL/6 mice showing TBI lesion 24h-post injury (A). Mild TBI was modelled using a controlled cortical impactor. 30-minutes post-TBI, mice were intravenously administered a vehicle or C-176. Sham mice underwent identical surgery omitting the TBI. Mice administered C-176 post-TBI had significantly reduced lesion volumes 24h after injury (*p=0.01) (B). Data represents mean ± SEM, n=8-9 animals per group.

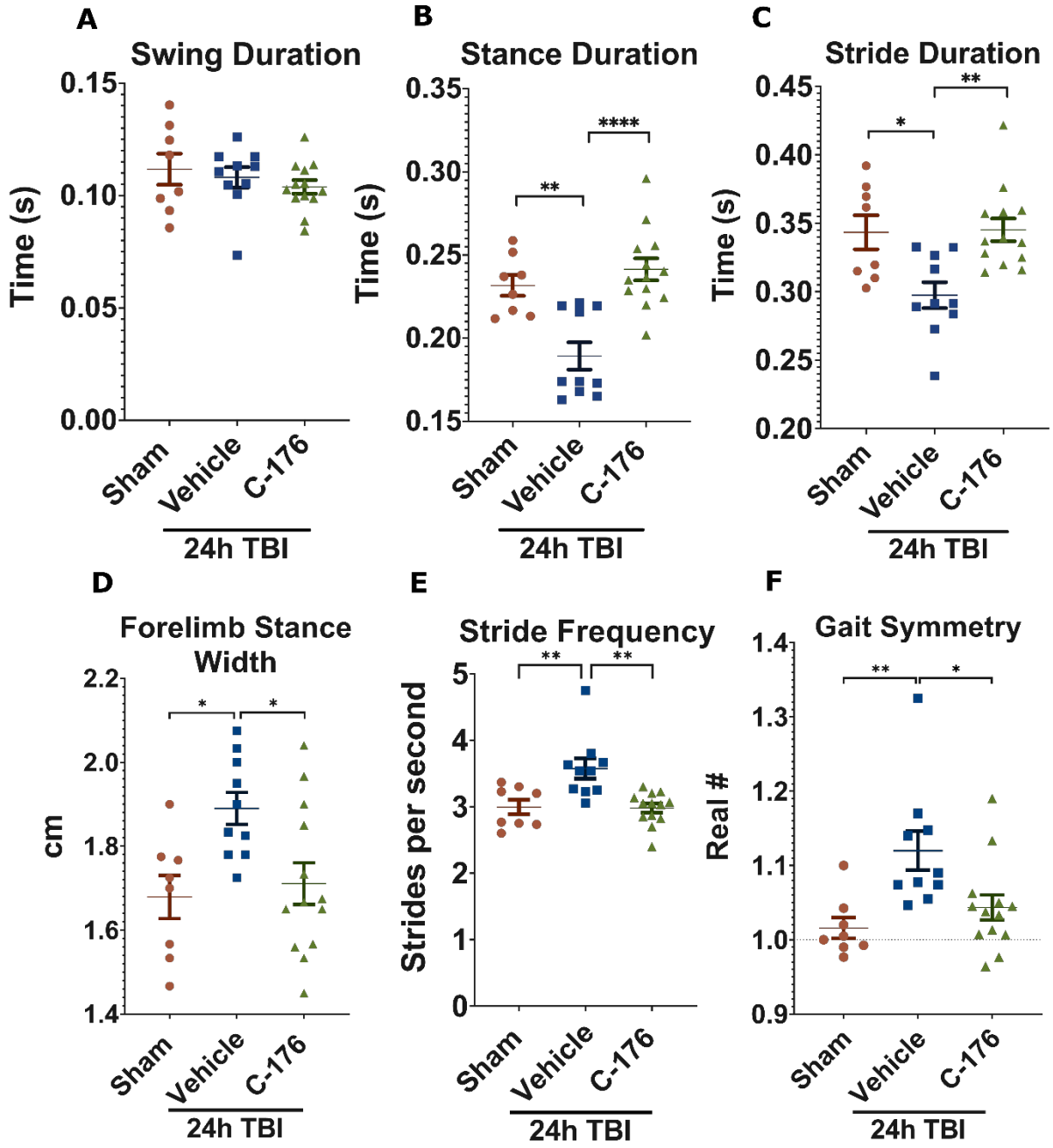

Figure 3. C-176 significantly improves left forelimb gait deficits 24h post-TBI.

Quantitative temporal gait parameters of mice were measured using DigiGait™ imaging and analysis software 24h after 1.5mm impact CCI surgery (TBI) and no impact (sham). No change in (A) swing duration was observed. Significant improvements found in (B) stance ($p<0.0001$) and (C) stride duration ($p=0.0032$), (D) stride frequency ($p=0.0011$), (E) forelimb stance width ($p=0.0254$) and (F) gait symmetry ($p=0.0237$) in TBI mice treated with STING inhibitor (C-176) compared to TBI mice treated with a vehicle. Sham n = 8, TBI-vehicle n = 10, TBI-C-176 n = 13. Data is presented as mean ± SEM. Significance determined by one-way ANOVA with Tukey's multiple comparison test. *P< 0.05, **P<0.01, ***P<0.001, ****P<0.0001.

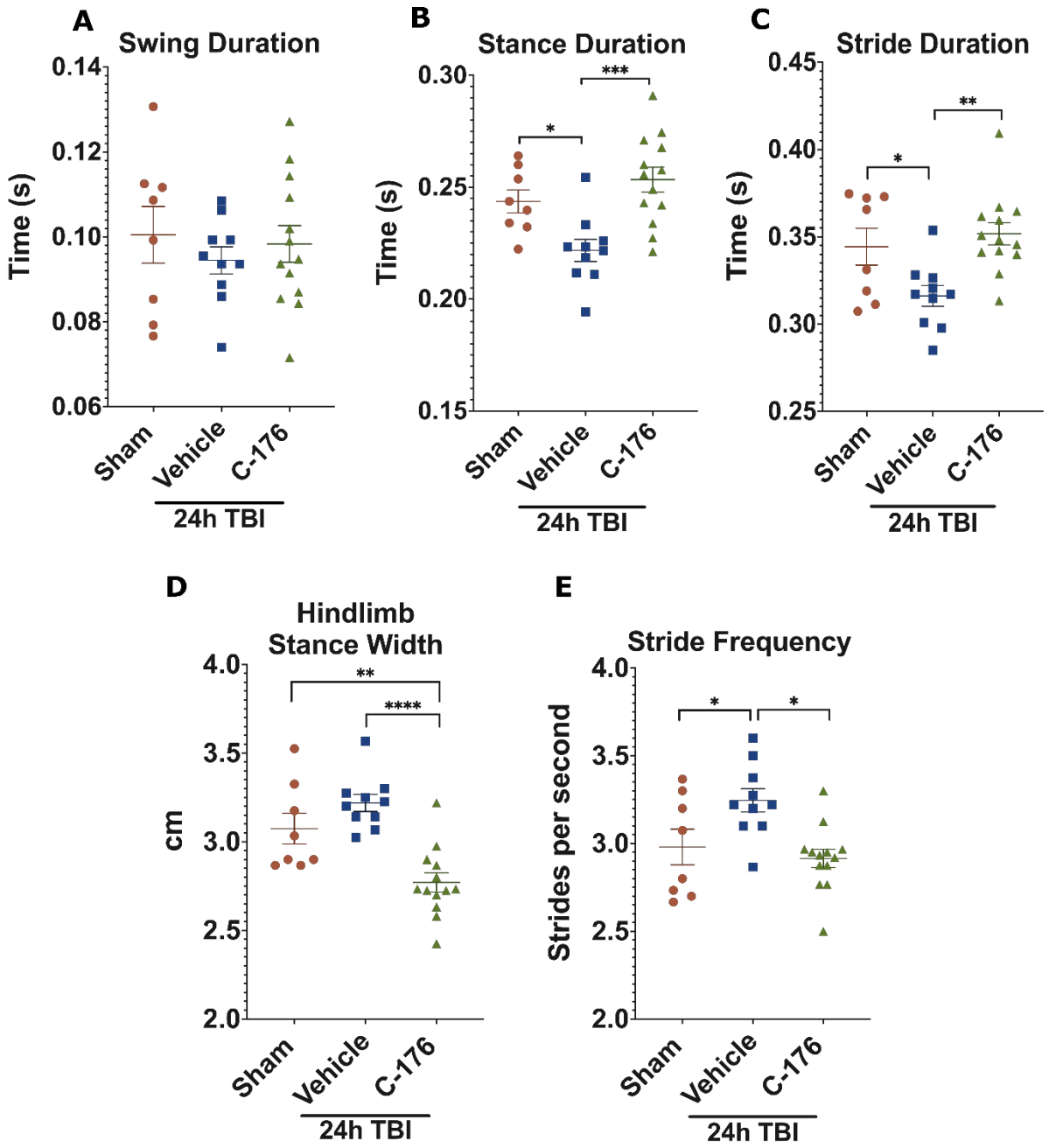

Figure 4. C-176 significantly improves left hindlimb gait deficits 24h post-TBI.

Quantitative temporal gait parameters of mice were measured using DigiGait™ imaging and analysis software 24h after 1.5mm impact CCI surgery (TBI) and no impact (sham). No change in swing duration between treatment groups was observed (A). Significant improvements found in (B) stance (p=0.0005) and (C) stride duration (p=0.0037), and (E) stride frequency (p=0.0041) in TBI mice treated with STING inhibitor (C-176) compared to TBI mice treated a vehicle. (D) Hindlimb stance width in C-176 treated mice significantly lower than sham (p=0.0052) and vehicle treated TBI mice (p<0.0001). Sham n = 8, TBI-vehicle n = 10, TBI-C-176 n = 13. Data is presented as mean ± SEM. Significance determined by one-way ANOVA with Tukey's multiple comparison test. *P< 0.05, **P<0.01, ***P<0.001, ****P<0.0001

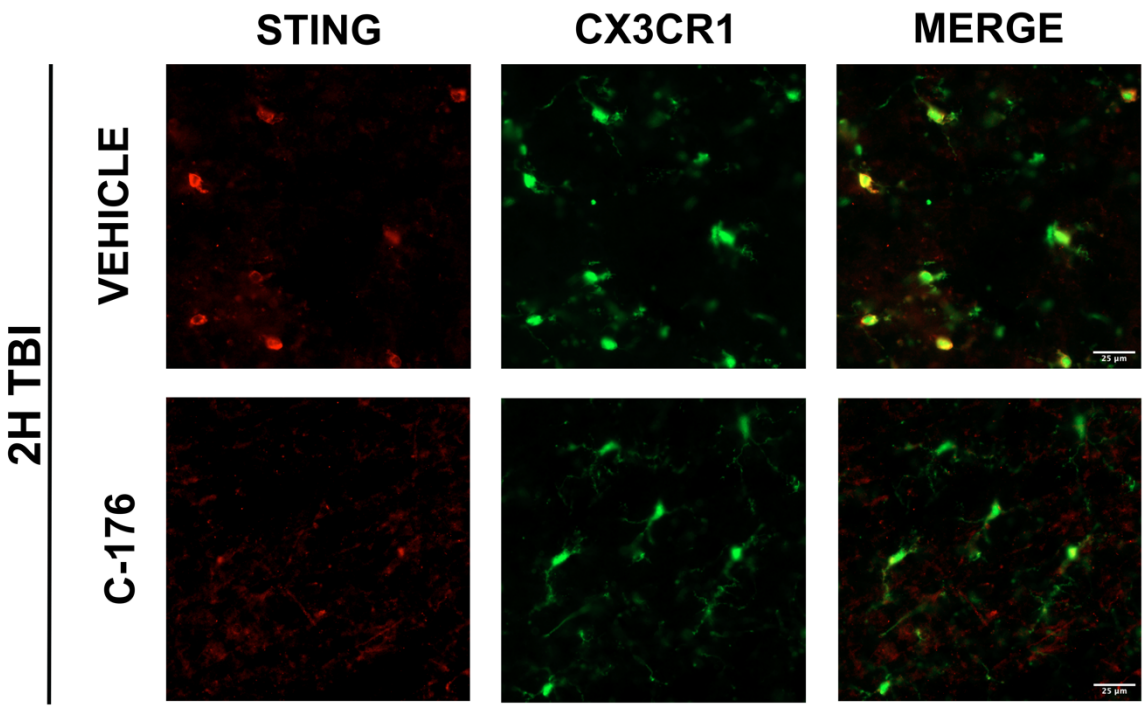

Figure 5. STING expression colocalises with microglia 2h-post TBI.

Representative immunofluorescence images of STING (red) and GFP-tagged CX3CR1 microglia (green) taken around lesion area 2h-post TBI. 30 minutes following TBI, mice were administered a saline vehicle (A) or a single dose of C-176 (B). Images taken on Zeiss Axio Observer 7.1 widefield microscope at 20X objective. Scale bar: 25µm

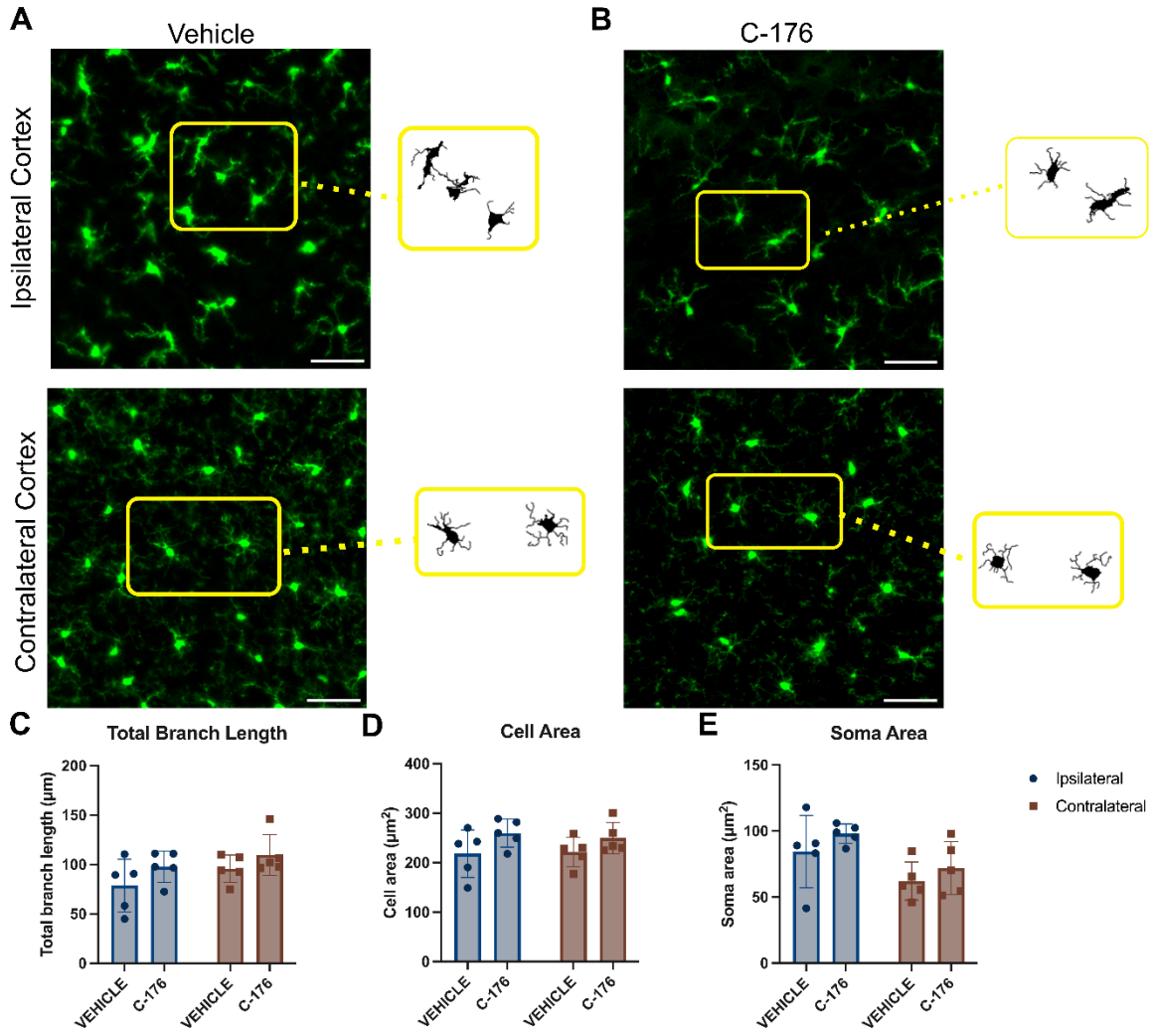

Figure 6. Administration of C-176 does not alter microglial morphology 24h-post TBI.

30µm thick brain sections of CX3CR1^{eGFP} mice subjected to CCI TBI. Representative images are shown for the ipsilateral and contralateral cortex of vehicle-treated (A) and C-176-treated (B) mice with an overview of the skeletonising process employed using a minimum spanning tree algorithm to measure morphological characteristics. Administration of C-176 did not significantly alter (C) total branch length (D), cell area or (E) soma area of perilesional microglia compared to vehicle treated mice 24h-post TBI. Each data point is an average of 200-500 cells. Scale bar = 50µm. n=5 for each group.

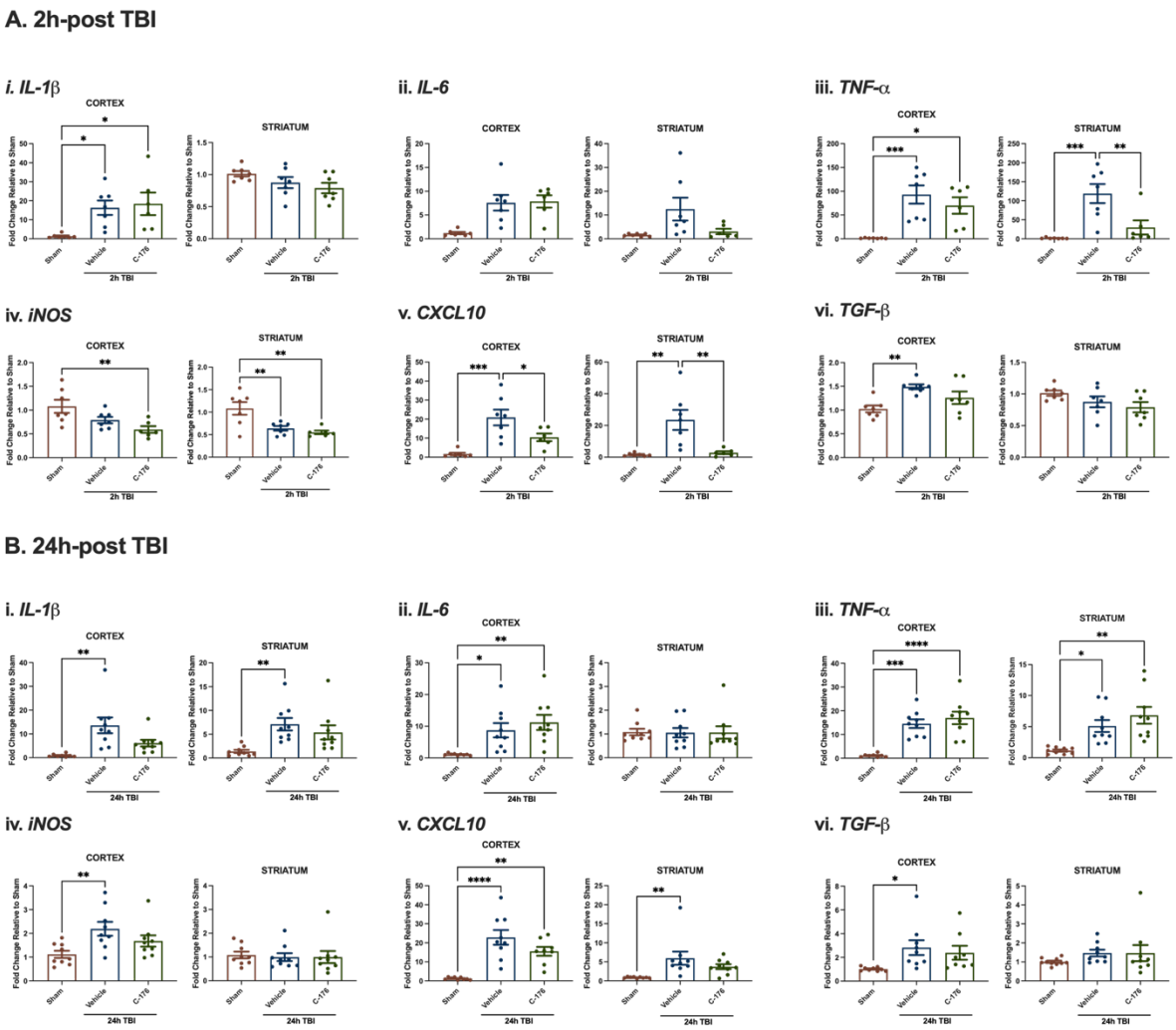

Figure 7. Gene expression of pro-inflammatory markers 2h and 24h following TBI and C-176 administration in mice.

Gene expression as measured by qPCR of pro-inflammatory markers in the ipsilateral cortex and striatum isolated 2h- (A) and 24h-post controlled-cortical impact modelled TBI (B) and intravenous administration with C-176 or a saline vehicle. 2h-post TBI (A), a significant increase in the cortical expression of *IL-1β* (i), *TNF-α* (iii), *CXCL10* (v) and *TGF-β* (vi) was observed. No significant change in the expression of *Il-6* (ii) was found. C-176 treated mice had significant attenuation of iNOS expression compared to sham in the cortex and striatum (iv) and significantly reduced expression of CXCL10 (v) compared to vehicle treated mice in the cortex (p=0.044) and striatum (p=0.0046). 24h-post TBI (B), vehicle-treated mice increased cortical expression of *IL-1β* (i), *IL-6* (ii), *iNOS* (iv) and TGF-*β* (iii). C-176 treated mice displayed an increase in the expression of TNF-*α* (iii) in the cortex and striatum and CXCL10 in the cortex (v). All data is presented as mean ± SEM. 2h-TBI n=6, 24h-TBI n = 9. Significance was determined for the cortex and striatum separately using a one-way ANOVA and Tukey's multiple comparison test. *p ≤ 0.05, **p ≤ 0.01, ***p ≤ 0.001, ****p < 0.0001.

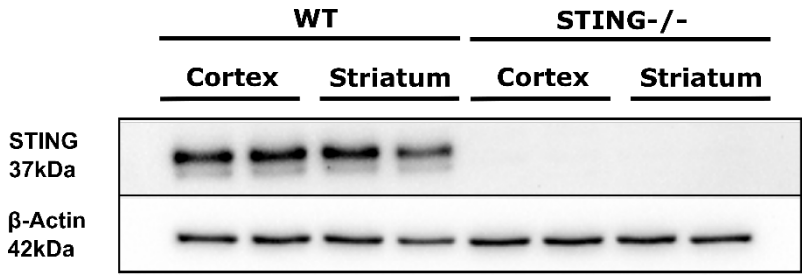

Supplementary figure 1. Validation of STING antibody

Brain lysate extracted from isolated cortex or striatum of wildtype (WT) or STING$^{-/-}$ C57Bl/6 mice. Total STING expression was detected using western blot. A single band was observed at approximately 37kDa in the WT lanes and was absent in STING$^{-/-}$

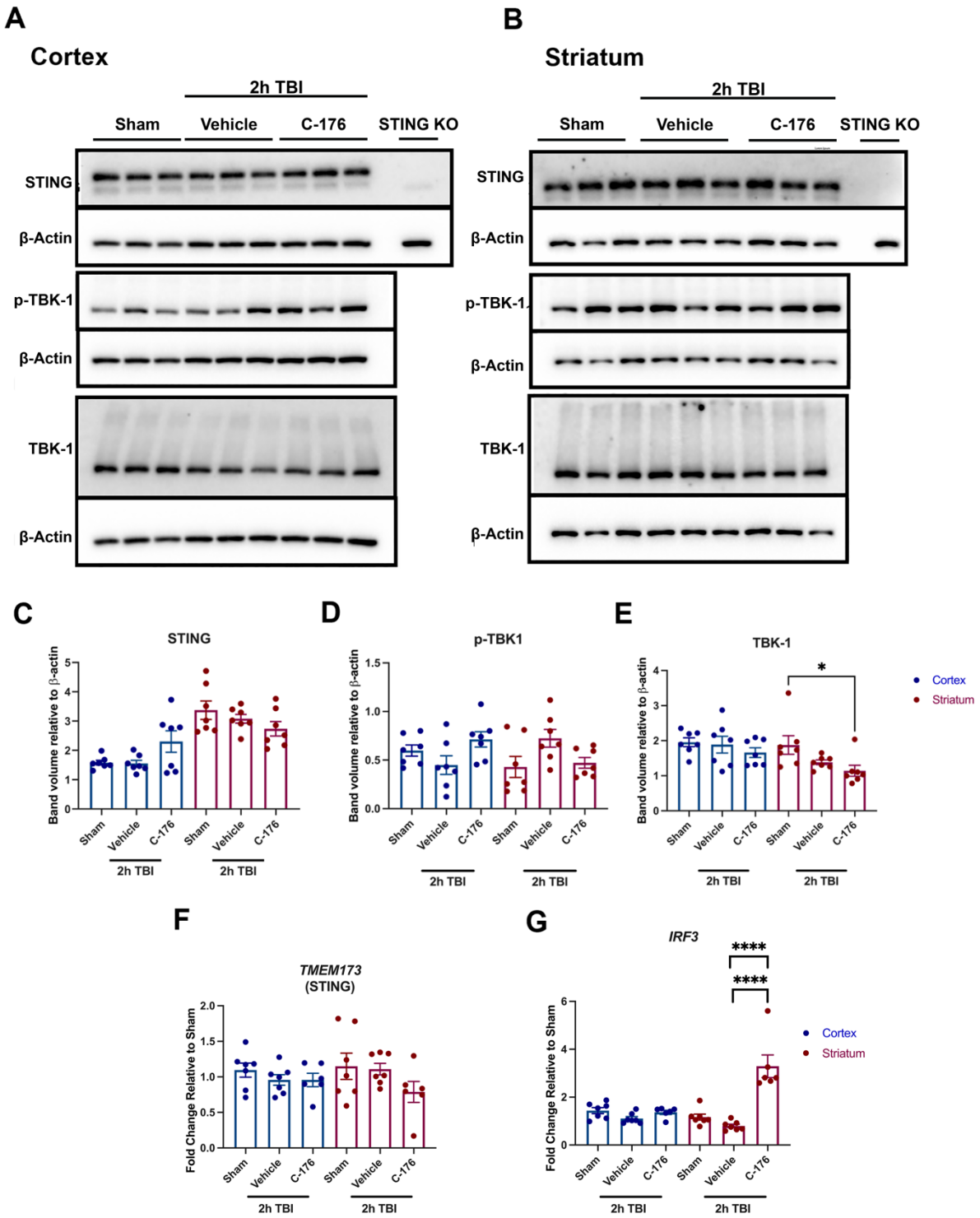

Supplementary Figure 2. STING, TBK1 and IRF3 expression 2h post-TBI and C-176 administration.

Representative images of STING, p-TBK1 and TBK1 protein expression the ipsilateral cortex and striatum of mouse brains 2h after controlled-cortical impact modelling of TBI or sham surgery as detected by western blot (A-B). Quantification of total STING (C), phospho-TBK1 (D) and total TBK1 (E) protein expression relative to β-actin loading control. No significant changes in the expression of (C) STING and (D) p-TBK1 were observed following TBI and C-176 administration compared to sham mice. TBI-mice treated with C-176 had a significantly lower expression of (E) total TBK1 compared to sham mice ($p=0.026$). Gene expression analysis by qPCR revealed no significant changes in the expression of TMEM173 (F) in the ipsilateral cortex and striatum and IRF3 (G) in the ipsilateral striatum 2h-post TBI. TBI-mice treated with C-176 had significantly elevated IRF3 expression compared to sham ($p<00001$) and vehicle-treated TBI-mice ($p<0.00001$). All data is expressed as mean ± SEM. Significance determined using a one-way ANOVA with Tukey's multiple comparison test. **p ≤ 0.01, *** p ≤ 0.001. n = 7 for each treatment group.

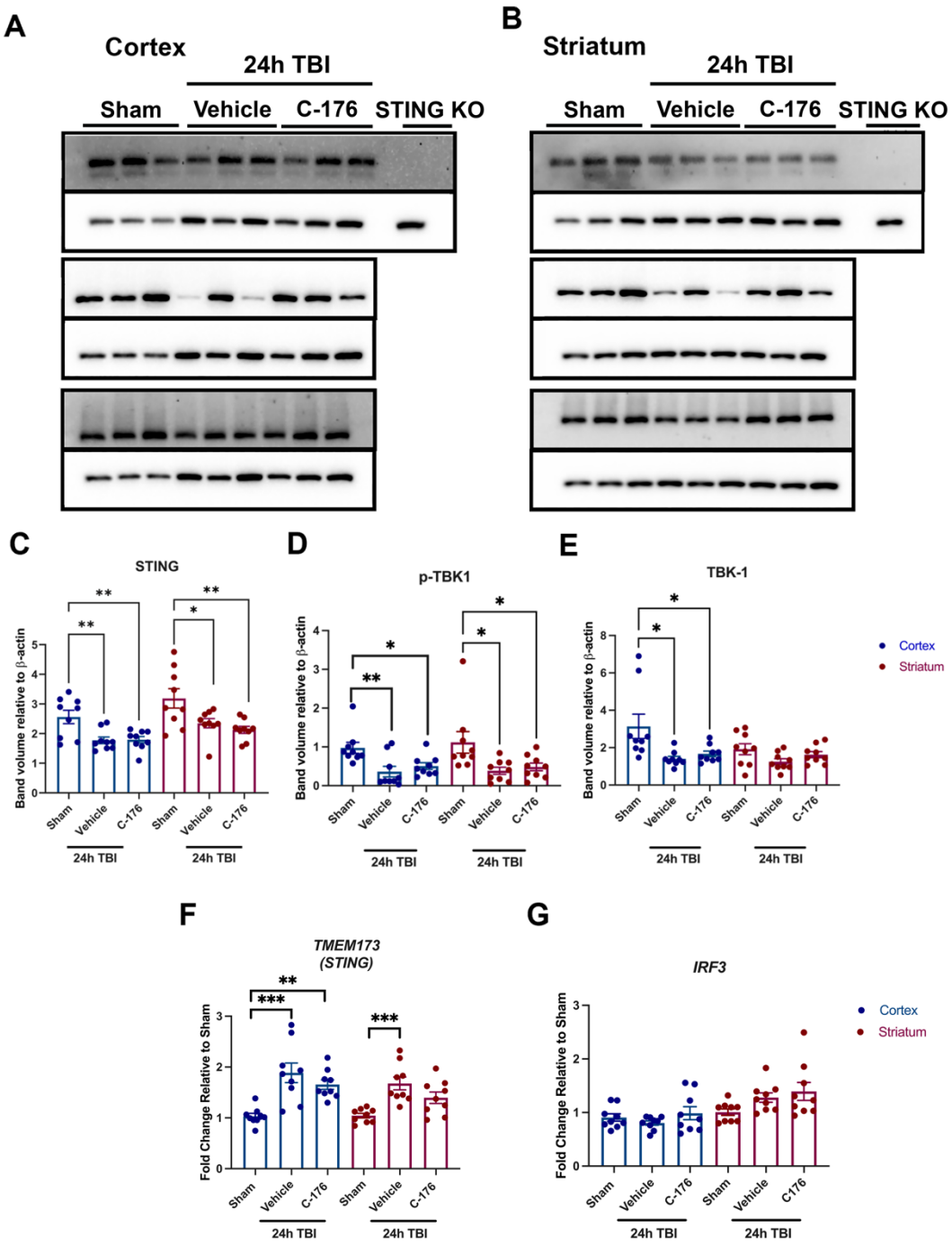

Supplementary Figure 3. STING, TBK1 and IRF3 expression 24h post-TBI and C-176 administration.

Representative images of STING, p-TBK1 and TBK1 protein expression the ipsilateral cortex and striatum of mouse brains 24h after controlled-cortical impact modelling of TBI or sham surgery as detected by western blot (A-B). Quantification of total STING (C), phospho-TBK1 (D), and total TBK1 (E) protein expression relative to β-actin loading control. Protein expression of STING (C) was significantly decreased in the cortex and striatum of TBI mice treated with vehicle (cortex p=0.0050, striatum p=0.0335 and C-176-treated mice (cortex p=0.0062, striatum p=0.0064) when compared to sham mice 24h-post TBI. No significant difference was observed in the expression of STING between the vehicle-treated and the C-176 treated TBI mice. P-TBK1 expression was significantly decreased in the cortex and striatum of both the vehicle-treated (cortex p=0.0054, striatum p=0.0202) and the C-176 treated mice (cortex p=0.0350, striatum p=0.0480) compared to sham mice. Gene expression analysis by qPCR revealed an increased expression of TMEM173 (F) 24h-post TBI in the cortex of both the vehicle treated mice (p=0.0002) and the C-176 treated mice (p=0.0057) compared to sham. Vehicle treated mice also displayed an increased expression of TMEM173 (p=0.0005). No significant change in the expression of IRF3 (G) was detected between all treatment groups. All data is expressed as mean ± SEM. Significance determined using a one-way ANOVA with Tukey's multiple comparison test. **p ≤ 0.01, *** p ≤ 0.001. n = 9 for each treatment group.

Table 1. Definition of DigiGait parameters

Gait parameter	Definition	Unit of measurement	Use in mouse models of traumatic brain injury (TBI) or spinal cord injury (SCI)
Swing duration	Time duration of the paw is off the treadmill (swing phase).	Seconds (s)	Ek et al. (2010); Neumann et al. (2009); Sashindranath et al. (2015)
Stance duration	Duration of paw contact with treadmill (stance phase)	Seconds (s)	Neumann et al. (2009); Sashindranath et al. (2015)
Stride duration	Time taken to complete one stride	Seconds (s)	Neumann et al. (2009); Sashindranath et al. (2015)
Stride frequency	The number of strides a paw completes each second. Also known as “cadence”.	Strides per second	Krizsan-Agbas et al. (2014); Sashindranath et al. (2015)
Stance width	The width between the forelimb or hindlimbs at peak stance. Also referred to as “base of support”.	cm	Ek et al. (2010); Krizsan-Agbas et al. (2014)
Gait symmetry	Ratio of forelimb stepping frequency to hind limb stepping frequency. A metric for co-ordination. Healthy mice should have a ratio close to one.	Real #	Krizsan-Agbas et al. (2014)

Supplementary Table 1. Primary antibodies used for western blot analysis

Primary antibody	Host Species	Dilution	Supplier	Catalogue number
STING *(in vivo)*	Rabbit	1:2000	Abcam	Ab288157
STING *(in vitro)*	Rabbit	1:1000	Cell Signalling Technologies	13647
Phospho STING	Rabbit	1:1000	Cell Signalling Technologies	72971
Anti-NAK/TBK1	Rabbit	1:1000	Abcam	Ab227182
Anti-NAK/TBK1 (phospho S172)	Rabbit	1:1000	Abcam	Ab109272
Anti-beta actin	Mouse	1:10000	Sigma-Aldrich	A5441

Supplementary Table 2. Secondary antibodies used for western blot analysis

Secondary antibody	Host Species	Dilution	Supplier	Catalogue number
Anti-rabbit immunoglobulins/HRP	Goat	1:1000	Dako Denmark	P0448
Anti-mouse immunoglobulins/HRP	Goat	1:1000	Dako Denmark	P0447

Supplementary Table 3. TaqMan primers used for qPCR analysis

Gene	Species	Refseq	Amplicon size (bp)	TaqMan Assay ID
GAPDH	Mouse	NM_008084.2	107	Mm99999915_m1
TMEM173 (STING)	Mouse	NM_028261.1	173	Mm0115817_m1
TNFα	Mouse	NM_013693.3	81	Mm00443258_m1
IRF3	Mouse	NM_016849.4	59	Mm00516779_m1
IL-6	Mouse	NM_031168.1	78	Mm00446190_m1
IL-1β	Mouse	NM_008361.3	63	Mm01336189_m1
CXCL10	Mouse	NM_021274.2	59	Mm00445235_m1

Supplementary Table 4. SYBR primers used for qPCR analysis

Gene	Forward primer (5’3’)	Reverse primer (5’3’)
GAPDH	ATCTTCTTGTGCAGTGCCAGC	ACTCCACGACATACTCAGCACC
iNOS	CAAGCACCTTGGAAGAGGAG	AAGGCCAAACACAGCATACC

Supplementary Table 5. Primary antibodies used for immunohistochemistry

Primary antibody	Host Species	Dilution	Supplier	Catalogue number
STING	Rabbit	1:500	Novus Biologicals	NBP2-24683

Supplementary Table 6. Secondary antibodies used for immunohistochemistry

Secondary antibody	Conjugate	Dilution	Supplier	Catalogue number
Goat anti-rabbit IgG	Alexa Fluor 594	1:1000	Invitrogen	A-11012